Spiral pattern in a radial displacement involving a reaction-producing gel

Yuichiro Nagatsu, Atsushi Hayashi, Mitsumasa Ban, Yoshihito Kato, and Yutaka Tada
Department of Materials Science and Engineering, Graduate School of Engineering, Nagoya Institute of Technology, Gokiso-cho, Showa-ku, Nagoya, Aichi, 466-8555, Japan

(Received 29 April 2008; revised manuscript received 30 June 2008; published 26 August 2008)

We have shown experimentally that the pattern created by the displacement of a more viscous fluid by a less viscous one in a radial Hele-Shaw cell develops not radially but spirally when a more viscous sodium polyacrylate solution is displaced by a less viscous trivalent iron ion (Fe^{3+}) solution with a sufficiently high concentration of Fe^{3+}. Another experiment revealed that an instantaneous chemical reaction takes place between the two fluids, and at high Fe^{3+} concentrations it produces a film of the gel at the contact plane. The gel film is proposed to be responsible for the spiral pattern.

DOI: 10.1103/PhysRevE.78.026307 PACS number(s): 47.54.−r, 82.40.Ck, 47.70.Fw, 47.20.Ma

I. INTRODUCTION

When a more viscous fluid is displaced by a less viscous fluid in porous media and in Hele-Shaw cells, the interface or boundary of the two fluids becomes unstable and forms a fingerlike pattern. This phenomenon is referred to as viscous fingering. Since the pioneering work on the fluid mechanics of viscous fingering published in the 1950s [1], many experimental and theoretical studies have been performed and some review articles have been published [2,3]. With respect to Newtonian fluids, this issue is well understood. There are two classes of viscous fingering: fingers formed in immiscible systems and those formed in miscible systems. The dimensionless number that controls the fingering dynamics in immiscible systems is the capillary number, which is defined as the ratio between viscous and interface-tension forces. In miscible systems, the dimensionless number is the Péclet number, which is defined as the ratio between convective and diffusive transport rates of mass [2]. In both systems, nonlinear propagation of viscous fingering is governed by the three mechanisms of shielding, spreading, and splitting. Shielding is the phenomenon in which a finger slightly ahead of its neighboring fingers quickly outruns them and shields them from further growth. Spreading and splitting are the phenomena in which a finger that spreads until it reaches a certain width becomes unstable and splits [2]. Viscous fingering has been frequently studied in a radial geometry in which the less viscous fluid is injected at an injection point and the fingering develops in a radial direction. We can see early experimental results of viscous fingering for Newtonian fluids in a radial Hele-Shaw cell in the studies done by Paterson for the immiscible [4] and miscible [5] cases.

We know from Nittmann, Daccord, and Stanley [6] that the non-Newtonian properties of the more viscous fluids have significant effects on the viscous fingering pattern. Experiments using some non-Newtonian fluids have revealed branched fractal or fracturelike patterns. Branched fractal and fracturelike patterns in a radial Hele-Shaw cell were demonstrated, for example, by Daccord, Nittmann, and Stanley [7] and Zhao and Maher [8], respectively. We also know that the viscous fingering pattern is changed by the anisotropy of the Hele-Shaw cell, as demonstrated by the research by Ben-Jacob *et al.* [9], who performed immiscible viscous fingering experiments in a radial Hele-Shaw cell by engraving a sixfold-symmetric network of channels of the same size on one of the plates. They observed the absence of a fingering pattern, six fingers growing along the six axes of the network but splitting later, six needle-shaped fingers growing along the axes without splitting or side branching, and six dendritic fingers growing along the axes with side branches, depending on the flow rate. The viscous fingering pattern is also changed by chemical reactions taking place between the more and less viscous fluids. Fernandez and Homsy [10] performed experiments on immiscible viscous fingering in a radial Hele-Shaw cell with a chemical reaction, which reduced the interfacial tension. In this case, the reaction widened the finger width. Nagatsu *et al.* [11] performed experiments on miscible viscous fingering with instantaneous chemical reactions acting to increase or decrease the viscosity of the more viscous fluid in a radial Hele-Shaw cell. In the case in which the viscosity was increased by the reaction, the shielding effect was suppressed and the finger was widened. In contrast, in the case in which the viscosity was decreased, the shielding was enhanced and the finger was narrowed.

As mentioned above, viscous fingering patterns in Hele-Shaw cells are changed by non-Newtonian properties, the anisotropy of the cell, and chemical reactions. In the radial geometry, nevertheless, viscous fingering patterns always develop in a radial direction, as observed so far. Here we describe the results of a viscous fingering experiment in a radial Hele-Shaw cell when using an aqueous sodium polyacrylate (SPA) solution as the more viscous fluid and a trivalent iron ion (Fe^{3+}) solution as the less viscous fluid. We show that the displacement pattern develops not radially but spirally, without fingering, under certain experimental conditions, although the pattern develops ordinarily in the radial direction under other experimental conditions. SPA is an anionic polymer with a large number of charges along the polymer chains. When a salt solution involving a divalent or trivalent cation is added to the SPA solution, depending on the salt concentration, the polymer chains are cross linked through the cation, gel is produced, and the liquid phase viscosity of the mixture decreases [12]. These are firmly established facts regarding the equilibrium state. However, our understanding of the nonequilibrium state, i.e., what happens when the SPA solution and the solution of the salt come into

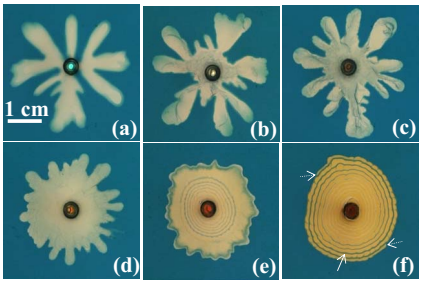

FIG. 1. (Color online) Displacement patterns for various $c_{Fe^{3+}}$. $c_{Fe^{3+}}$=(a) 0, (b) 0.001M, (c) 0.01M, (d) 0.1M, (e) 1M, and (f) 4M. The meaning of the arrow with a solid line and of arrows with dotted lines is presented in the text.

contact and mix, is sparse. In the present study, we conducted a separate experiment to obtain information regarding this issue. We discuss a mechanism of spiral pattern formation based on the results of this experiment.

II. EXPERIMENTAL SETUP

In the present study, viscous fingering experiments were conducted by using a radial Hele-Shaw cell. This apparatus is the same as that used in our previous study [11]. The gap width b was set at $b=0.5$ mm. The SPA used in the present study is manufactured by Wako, Japan, and has a molecular weight of $(2.1-6.6)\times 10^6$. The experimental results were obtained by using $Fe(NO_3)_3$ solution as the solution including Fe^{3+}. We also used $FeCl_3$ solution and confirmed that similar results mentioned later were obtained, although the results obtained by using the $Fe(NO_3)_3$ and the $FeCl_3$ solutions were somewhat different quantitatively. In viscous fingering experiments where both the less and more viscous fluids are liquids, it is customary to dye the less viscous liquid. In the present study, however, the more viscous liquid, i.e., the SPA solution, was dyed blue using indigo carmine because it was difficult to find dye for the Fe^{3+} solution. The concentration of the indigo carmine was set at 0.1 wt %. We confirmed that the viscosity of the SPA solution decreased somewhat with the addition of the indigo carmine. The Fe^{3+} solution is light yellow, and the color deepens with increase in the concentration of Fe^{3+}. The present system is a miscible one, and thus we have to define the Péclet number Pe. In the radial Hele-Shaw geometry, it is common to define Pe as $Pe=q/2\pi bD$ [11,13], and that was the definition we employed in the present study. In this definition, q is the injection rate of the less viscous liquid, and D is the diffusion coefficient between the more and less viscous liquids, which we estimated to be 1×10^{-9} m^2/s, because in the present system D could be regarded as the diffusion coefficient of the polymer at small concentrations in water [11]. Experiments were conducted by varying the concentration of Fe^{3+}, $c_{Fe^{3+}}$, the concentration of SPA, c_{SPA}, and Pe (or q).

III. RESULTS

A. Conditions for observing the spiral pattern

Figure 1 shows the displacement patterns for various $c_{Fe^{3+}}$ under conditions where $c_{SPA}=0.75$ wt % and $Pe=1.5\times 10^3$ ($q=4.5\times 10^{-9}$ m^3/s), at $t=120$ s, where t is the injection time of the less viscous liquid. When (a) $c_{Fe^{3+}}=0$, a viscous fingering pattern is observed. When $c_{Fe^{3+}}$=(b) 0.001M, and (c) 0.01M, a slight difference in the fingering pattern can be observed compared to the case of $c_{Fe^{3+}}=0$, in which the area occupied by the less viscous liquid around the injection hole is larger and fingering occurs at a larger radius, with an increase in $c_{Fe^{3+}}$. When $c_{Fe^{3+}}$=(d) 0.1M and (e) 1M, the difference in the fingering pattern compared to the case of $c_{Fe^{3+}}=0$ is pronounced, as fingering occurs at a significantly larger radius and thus the pattern approaches a circularlike pattern with an increase in $c_{Fe^{3+}}$. When $c_{Fe^{3+}}=1M$, a circularlike pattern is observed. When (f) $c_{Fe^{3+}}=4M$, the pattern becomes completely circular and no fingering can be observed. In this case, annular blue inclusions can be observed in a circular yellow region. Surprisingly, the pattern develops not in a radial direction but spirally. The arrow with the solid line indicates one of the blue lines in the yellow region which delimits the spiral pattern. Arrows with dotted lines indicate the tips of the displacement. Note that, in the yellow region with small radius, the annular lines are visible as light yellow lines rather than as blue lines. However, at earlier times, clear blue annular lines can be observed in this region. It should be noted that the blue annular pattern can be observed in a region with a small radius when $c_{Fe^{3+}}=1M$. In this case, the pattern develops spirally at an early stage. After the spiral completely stops, the pattern develops in the radial direction. A movie of the formation of a clear spiral pattern can be seen at [14] in which a 4M Fe^{3+} solution displaces 0.75 wt % SPA solution without the dye at $Pe=1.5\times 10^3$. In the movie, a clear spiral pattern that develops only counterclockwise can be observed.

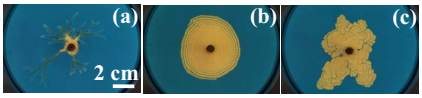

FIG. 2. (Color online) Displacement patterns for various Pe. Pe=(a) 2.9×10^2 (at $t=210$ s), (b) 1.5×10^3 (at $t=210$ s), and (c) 1.5×10^4 (at $t=24$ s).

The typical effects of Pe on the present system are shown in Fig. 2. Figures 2(a)–2(c) show the displacement patterns for various Pe under the conditions of $c_{SPA}=0.75$ wt % and $c_{Fe^{3+}}=4M$. For intermediate Pe, the spiral pattern is formed [Fig. 2(b)]. For low Pe, the fingering pattern is observed [Fig. 2(a)]. In other words, the pattern develops in a radial direction. For high Pe, the pattern develops totally in the radial direction, but the pattern involves a multiplicity of small spirals locally [Fig. 2(c)]. These results show that the spiral pattern is formed only in the intermediate range of Pe. It should be noted that in the fingering pattern in Fig. 2(a), the color of the Fe^{3+} solution is very light, which indicates that the Fe^{3+} solution cannot completely displace the SPA solution in the cell's gap direction. In contrast, the color of the Fe^{3+} solution is deep in Figs. 2(b) and 2(c), which, in turn, indicates that the Fe^{3+} solution can completely displace the SPA solution in the cell's gap direction.

Figure 3 shows the classification of the displacement pattern for various $c_{Fe^{3+}}$ and Pe conditions under the condition

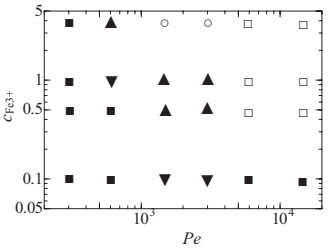

FIG. 3. Diagram for classification of the displacement pattern under the condition c_{SPA}=0.75 wt %. The meanings of the symbols are given in the text.

of c_{SPA}=0.75 wt %. In the diagram, ○ indicates that the spiral pattern forms stably for a long time as in Fig. 1(f); ▲ indicates a pattern like that in Fig. 1(e), where the spiral forms during the initial stage but does not remain as time proceeds; ▼ indicates a pattern without the formation of a spiral, like that in Fig. 1(d). Also, ■ indicates a fingering pattern like that in Fig. 2(a), i.e., a fingering pattern involving incomplete displacement in the cell's gap direction, while □ indicates a pattern like that in Fig. 2(c) involving multiple small spirals. The diagram confirms that a spiral pattern is stably formed for conditions of high $c_{Fe^{3+}}$ and intermediate Pe.

The effects of c_{SPA} on the present system are shown in Fig. 4. Figures 4(a)–4(c) show the displacement patterns for various c_{SPA} under the conditions of $c_{Fe^{3+}}=4M$ and Pe=1.5 $\times 10^3$ at t=130 s. For c_{SPA}=0.5 wt %, the pattern develops in the radial direction, although clear fingering does not occur. For both c_{SPA}=0.75 and 1.25 wt %, a spiral pattern is formed; however, that for c_{SPA}=1.25 wt % is broken at an early phase. This indicates that the spiral pattern is formed most stably under intermediate c_{SPA}.

B. Properties of the spiral

We have investigated which factors determine the width of an "arm" of the spiral and the gap between the arms. Figures 5(a)–5(c) show the spiral pattern for various Pe under the conditions of c_{SPA}=0.75 wt % and $c_{Fe^{3+}}=4M$, where the SPA solution is not dyed. As shown, the width of an arm hardly depends on Pe, but the gap between the arms is wider with a decrease in Pe. Note that we have found that the width of the arm and the gap between the arms are independent of $c_{Fe^{3+}}$ and c_{SPA} (not shown).

IV. DISCUSSION

A. Another experiment to examine the process of mixing and chemical reaction between the SPA solution and the Fe^{3+} solution

To investigate the mechanism of the spiral pattern formation, we have examined what happens when the SPA and Fe^{3+} solutions come into contact and then mix under the presence of fluid shear by means of another experiment. In the experiment, the $Fe(NO_3)_3$ solution at a given concentration was dropped at 1 ml/s for 10 s into a beaker containing 30 ml of 0.625 wt % SPA solution that was stirred by a magnetic stirrer. The fluid motion in the beaker was observed during and after the dropping of the Fe^{3+} solution. In this experiment, the SPA solution was not dyed and was colorless. Figure 6 shows the observed results of the cases in which the concentration of Fe^{3+} is (a) 0.01M, (b) 0.1M, and (c) 1.2M at t=330 s. Here, t=0 s indicates the time when the Fe^{3+} solution begins to be dropped. In the case of 1.2M [Fig. 6(c)], surprisingly the two liquids remain separate, even though they are miscible and the density of the 1.2M Fe^{3+} solution (upper side) is larger than that of the 0.625 wt % SPA solution (lower side). This is caused by a film of gel formed by the reaction at the contact plane between the two liquids, which is hard enough to sustain the heavier 1.2M Fe^{3+} solution present in the upper side. In the cases of 0.1M [Fig. 6(b)] and 0.01M [Fig. 6(a)], the SPA solution and Fe^{3+} solution are mixed and the yellow material is gel produced by the reaction between the SPA solution and Fe^{3+} solution. This result indicates that the gel film in these cases is not hard enough to sustain the Fe^{3+} solutions present in the upper side. Note that the two liquids remain separate until t =120 s in the case of 0.1M [Fig. 6(b)], while the two liquids initially start to mix in the case of 0.01M [Fig. 6(a)]. More gel is formed in the case of 0.1M [Fig. 6(b)] than in the case of 0.01M [Fig. 6(a)]. The free surface of the liquid phase of the mixture is flat in the case of 0.01M [Fig. 6(a)], while that in the case of 0.1M [Fig. 6(b)] is significantly hollow. These results show that the viscosity of the liquid phase is significantly lower in the case of 0.1M [Fig. 6(b)] than in the case of 0.01M [Fig 6(a)]. In brief, the results of this experiment can be interpreted as follows. When the Fe^{3+} solution and the SPA solution come into contact, an instantaneous chemical reaction takes place which forms a gel film at the contact plane between the two liquids. The hardness of the film increases with the concentration of Fe^{3+}. Once the film is broken owing to fluid shear, mixing of the Fe^{3+} and the SPA solutions occurs and the chemical reaction again takes place, which produces the gel and decreases the mixture's liquid phase viscosity. With increasing concentration of Fe^{3+}, the quantity of gel produced increases and the decrease in the mixture's liquid phase viscosity becomes significant. We attempted to measure the hardness of the gel film, but we found that even extraction of the gel film was a truly daunting task because the film was significantly thin and very soft.

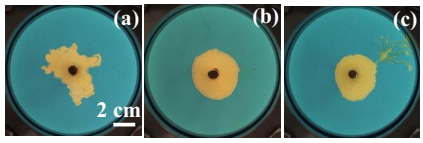

FIG. 4. (Color online) Displacement patterns for various c_{SPA}. c_{SPA}=(a) 0.5, (b) 0.75, and (c) 1.25 wt %.

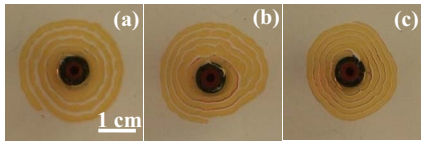

FIG. 5. (Color online) Spiral patterns for various Pe. Pe=(a) 2.9×10^2 (at t=180 s), (b) 5.8×10^2 (at t=90 s), and (c) 1.5×10^3 (at t=36 s).

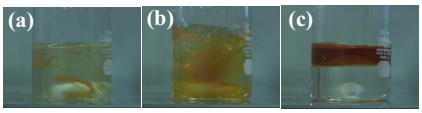

FIG. 6. (Color online) Flow behavior in a beaker after 10 ml $Fe(NO_3)_3$ solution at concentrations of (a) $0.01M$, (b) $0.1M$, and (c) $1.2M$ is dropped into a beaker containing 30 ml 0.625 wt % SPA solution stirred by a magnetic stirrer at $t=330$ s. The white objects on the bottom of the beaker are magnetic stirrers.

B. A proposed mechanism for the formation of the spiral pattern

Based on our experiments, we propose a physical model in which the film of the gel formed by the reaction between the SPA and Fe^{3+} solutions is responsible for the formation of the spiral pattern. Figure 7 shows schematics of the early stage of the spiral pattern. Initially at the injection hole, the gel is formed along the circumference of the injection hole [Fig. 7(a)]. After that, the less viscous liquid is ejected from one point [Fig. 7(b)]. This is considered to occur because the gel film formed by the reaction at the contact plane between the two liquids is hard enough to behave as a wall. The gel wall is likely to be broken at one point, and the less viscous liquid is ejected at the broken point rather than staying behind the circular wall of spreading gel. After the ejection, the less viscous liquid penetrates spirally [Fig. 7(c)]. When the one spiral penetration stops, the less viscous liquid is ejected at another point [Fig. 7(d)] and penetrates spirally again [Fig. 7(e)]. The ejection and spiral penetration processes are repeated, resulting in the formation of the spiral pattern. Since one spiral, in general, does not continuously develop, both clockwise and counterclockwise spirals can be observed in one experimental run. If spiral penetration does not stop, a spiral pattern develops only clockwise or only counterclockwise, as seen in the movie cited previously [14].

Here, the question arises as to why the less viscous liquid penetrates spirally and not radially after the ejection. The reason the authors propose is explained by the schematic in Fig. 8. If the less viscous liquid penetrates in the radial direction in the manner of a finger [Fig. 8(a)], the gel's film is newly formed at the tip of the finger and along both sides of the finger. When the less viscous liquid penetrates spirally [Fig. 8(b)], a new film of gel forms significantly at the tip and the outside of the arm of the spiral. These occurrences indicate that the amount of gel formed is smaller in the case of (b) than in the case of (a). Darcy's law [$\nabla p=-(\mu/K)\underline{u}$, where ∇p is the gradient of pressure, $\underline{u}$ is the velocity field, and μ and K are the viscosity and permeability, respectively], which accounts for momentum conservation in flows in porous media, suggests that it is easier for the fluid to move if its viscosity is lower for a given pressure gradient.

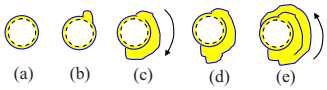

FIG. 7. (Color online) Schematics of the early stage of the spiral pattern. The black broken circle represents the injection hole. Blue solid lines indicate the gel film.

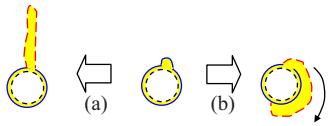

FIG. 8. (Color online) Schematics to explain why the less viscous liquid penetrates not radially but spirally after the ejection. Red long-dashed lines indicate the gel film newly formed after the ejection. The cases where the less viscous liquid penetrates radially and spirally are shown in (a) and (b), respectively.

Thus, since the gel film can be regarded as a fluid with very high viscosity, the less viscous liquid is considered to tend to penetrate in a manner that minimizes the amount of gel formed. We believe this is why the spiral pattern develops.

C. Explanation of the experimental results obtained

In Fig. 1 (effects of $c_{Fe^{3+}}$), the hardness of the gel film can be interpreted as varying according to $c_{Fe^{3+}}$ in the experiments. In the cases of Fig. 1(d) $c_{Fe^{3+}}=0.1M$ and Fig. 1(e) $c_{Fe^{3+}}=1M$, the nearly circular pattern is interpreted as induced by the boundary spreading as the length of the boundary is minimized because the gel film in this case is hard but not hard enough to cause the ejection of the less viscous liquid at one point. In the cases of Fig. 1(b) $c_{Fe^{3+}}=0.001M$ and Fig. 1(c) $c_{Fe_{3+}}=0.01M$, the gel film formed by the reaction is not so hard that a significant difference in the fingering pattern cannot be observed compared to the case of $0M$. The chemical reaction treated here has two effects. One is the formation of the gel, and the other is the decrease in the viscosity of the liquid phase of the mixture. In the viscous fingering experiments in Fig. 1, the latter effect probably did not take place, because we know from our previous study that the decrease in the viscosity of the more viscous liquid induced by the instantaneous reaction narrows the finger and enhances the shielding effects [11].

In the cases in Fig. 2 (effects of Pe), we believe the hardness of the gel film remaines unchanged because the hardness is determined by c_{SPA} and $c_{Fe^{3+}}$. The incomplete displacement of the less viscous liquid in the cell's gap direction for low Pe is caused by the displacement speed not being high enough for the less viscous liquid to uniformly push the gel film in the cell gap direction. At a low displacement speed the gel film is thought to be broken at the upper or lower contact point between the gel film and the glass plates of the cell because the gel film is mechanically weak-

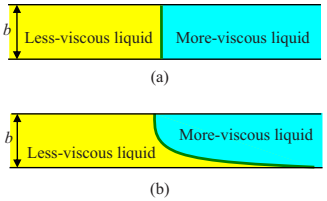

FIG. 9. (Color online) Schematics of the structure in the cell gap for (a) complete and (b) incomplete displacement of the less viscous liquid. The gel film formed at the contact plane between the more and less viscous liquids is indicated by a green line.

est there. This is shown schematically in Fig. 9(b), in which the lower contact point is drawn as broken because it is more likely to occur for this case due to the higher density of the less viscous liquid. The incomplete displacement is the probable reason why the spiral pattern cannot form in cases of low Pe. As is the case with intermediate Pe, complete displacement in the cell's gap direction takes place for high Pe, and thus the pattern tends to form a spiral. However, in this case the less viscous liquid is ejected in the radial direction before the clear spiral pattern is established. Therefore, a pattern with multiple small spirals develops in the radial direction.

In the cases shown in Fig. 4 (the effects of c_{SPA}), the viscosity of the more viscous SPA solution is higher with higher c_{SPA}. Also, the hardness of the gel film formed appears to be increased with increasing c_{SPA}. For $c_{\mathrm{SPA}}=0.5$ wt %, the color of the Fe^{3+} solution is deep, indicating that the Fe^{3+} solution can completely displace the SPA solution in the cell gap direction. In this case the viscosity of the more viscous liquid is not high and the gel film is not hard enough for the less viscous liquid to penetrate spirally, and thus the pattern can develop in the radial direction. The spiral pattern for $c_{\mathrm{SPA}}=1.25$ wt % breaks earlier than that for $c_{\mathrm{SPA}}=0.75$ wt % because the gel film is thought to be harder and the viscosity of the more viscous liquid is higher in the case of $c_{\mathrm{SPA}}=1.25$ wt % compared to the case of $c_{\mathrm{SPA}}=0.75$ wt %. We postulated that a moderately fast displacement speed is required to uniformly push the relatively hard gel film and the relatively higher-concentration more viscous liquid over the cell gap in the discussion of the case of low Pe in Fig. 2. Here, we additionally postulate that the required displacement speed increases as the gel's film is harder and the viscosity of the more viscous liquid is higher. Based on that postulation, the threshold of the displacement speed at which the less viscous liquid is not able to uniformly push the gel film and the more viscous liquid over the cell gap is larger for $c_{\mathrm{SPA}}=1.25$ wt % than for $c_{\mathrm{SPA}}=0.75$ wt %. This is why we believe the spiral pattern forms more stably for $c_{\mathrm{SPA}}=0.75$ wt % than for $c_{\mathrm{SPA}}=1.25$ wt %. The situation under which the spiral pattern cannot form because of a low displacement speed is similar to the case of low Pe in Fig. 2. In other words, the gel film is supposed be broken at the upper or lower contact point between the gel film and the glass plates of the cell, as shown in Fig. 9(b). Actually, after the break of the spiral pattern, the fingering pattern develops in the radial direction and the color of the Fe^{3+} solution is very light, like the case shown in Fig. 2(a). It should be noted that $c_{\mathrm{SPA}}=1.25$ wt % is the maximum limit to homogeneously mix the polymer with water. This means that above $c_{\mathrm{SPA}}=1.25$ wt % it is difficult to homogeneously mix the polymer solution because of the significantly high viscosity.

A reason for the increase in the gap between the arms with the decrease in Pe is proposed in Figs. 10(a) and 10(b). After the less viscous liquid is ejected from one point, it can penetrate for a longer distance in the radial direction for low Pe [Fig. 10(a)] than for high Pe [Fig. 10(b)]. This is considered to be because the less viscous liquid gradually displaces the more-viscous liquid for small Pe. In Fig. 8, we explain that the new film of gel forms significantly at the tip and the outside of the arm of the spiral when the less viscous liquid penetrates spirally. In the photograph in Fig. 5(a) as well as in the schematics in Fig. 10(a), for low Pe, the gel film is newly formed at the tip and along both sides of the arm. In this case, the gel film formed along the inside of the newly formed arm is thought to be softer than that formed along the outside of the newly formed arm. This is because the SPA in the more viscous liquid in the vicinity of the inside of the newly formed arm is somewhat consumed when the previously formed arm is created. Therefore, the amount of gel formed in spiral development like that depicted in Figs. 5(a) and 10(a) is considered to still be smaller than that present with the penetration of the less viscous liquid in the radial direction in the manner of a finger.

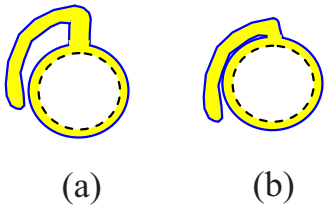

FIG. 10. (Color online) Schematics of the spiral development for (a) low and (b) high.

V. CONCLUSION

We show that the displacement pattern of a more viscous fluid by a less viscous fluid in a radial Hele-Shaw cell develops not radially but spirally when the SPA solution (the more viscous fluid) is displaced by a high-concentration Fe^{3+} solution (the less viscous fluid) under certain experimental conditions. We found that the spiral pattern is formed only for intermediate Pe. Regarding the concentration of SPA, c_{SPA}, for moderate c_{SPA} the spiral pattern is stably formed. In addition, we found that the arm's width of the spiral is independent of experimental parameters, but the gap between the arms increases with the decrease in Pe. Another experiment revealed that the reaction between the SPA solution and the Fe^{3+} solution takes place instantaneously and forms a gel film. The hardness of the film increases with the concentration of Fe^{3+}. We present a physical model in which the gel film is responsible for the spiral pattern. To our knowledge, this is the first instance in the history of the study of viscous fingering that shows a displacement pattern developing in a nonradial pattern in radial Hele-Shaw cells.

ACKNOWLEDGMENTS

This research was partially supported by the Research Foundation for Electrotechnology of Chubu, Japan. The authors are also grateful to Professor Shuichi Iwata, Nagoya Institute of Technology, for helpful discussion.

[1] S. Hill, Chem. Eng. Sci. **1**, 247 (1952); P. G. Saffman and G. I. Taylor, Proc. R. Soc. London, Ser. A **245**, 312 (1958); R. L. Chouke, P. van Meurs, and C. van der Pol, Trans. AIME **216**, 188 (1959).
[2] G. M. Homsy, Annu. Rev. Fluid Mech. **19**, 271 (1987).
[3] K. V. McCloud and J. V. Maher, Phys. Rep. **260**, 139 (1995); S. Tanveer, J. Fluid Mech. **409**, 273 (2000).
[4] L. Paterson, J. Fluid Mech. **113**, 513 (1981).
[5] L. Paterson, Phys. Fluids **28**, 26 (1985).
[6] J. Nittmann, G. Daccord, and H. E. Stanley, Nature (London) **314**, 141 (1985).
[7] G. Daccord, J. Nittmann, and H. E. Stanley, Phys. Rev. Lett. **56**, 336 (1986).
[8] H. Zhao and J. V. Maher, Phys. Rev. E **47**, 4278 (1993).
[9] E. Ben-Jacob, R. Godbey, N. D. Goldenfeld, J. Koplik, H. Levine, T. Mueller, and L. M. Sander, Phys. Rev. Lett. **55**, 1315 (1985).
[10] J. Fernandez and G. M. Homsy, J. Fluid Mech. **480**, 267 (2003).
[11] Y. Nagatsu *et al.*, J. Fluid Mech. **571**, 475 (2007).
[12] T. Nakamura, *Water Soluble Polymers*, enlarged ed. (Kagaku Kougyosha, Tokyo, 1981) (in Japanese).
[13] P. Petitjeans *et al.*, Phys. Fluids **11**, 1705 (1999).
[14] See EPAPS Document No. E-PLEEE8-78-178808 for a movie of the clear spiral pattern formation. The movie shown is in real speed. For more information on EPAPS, See http://www.aip.org/pubservs/epaps.html.